Hindawi
Shock and Vibration
Volume 2018, Article ID 2493149, 9 pages
https://doi.org/10.1155/2018/2493149

Research Article

Experimental Investigation of the Propagation and Attenuation Rule of Blasting Vibration Wave Parameters Based on the Damage Accumulation Effect

Huaibao Chu,[1,2] Xiaolin Yang,[1,2] Shuanjie Li,[1,2] and Weimin Liang[1,2]

[1]*College of Civil Engineering, Henan Polytechnic University, Jiaozuo 454000, China*
[2]*Henan Key Laboratory of Underground Engineering and Disaster Prevention, Jiaozuo 454000, China*

Correspondence should be addressed to Shuanjie Li; lishuanjie@qq.com

Received 31 May 2018; Revised 22 October 2018; Accepted 25 October 2018; Published 2 December 2018

Academic Editor: Marco Tarabini

The propagation and attenuation rule of blasting vibration wave parameters is the most important foundation of blasting vibration prediction and control. In this work, we pay more attention to the influence of the damage accumulation effect on the propagation and attenuation rule of vibration wave parameters. A blasting damage accumulation experiment was carried out, the ultrasonic wave velocity of the specimens was measured, and the damage value was calculated during the experiment. The blasting vibration wave was monitored on the surface of the specimens, and its energy was calculated by using the sym8 wavelet basis function. The experimental results showed that with the increase in the number of blasts, the damage continues to increase; however, the vibration velocity and the main frequency decrease continuously, the unfocused vibration wave energy in the zone near to the blasting source is rapidly concentrated in the low-frequency band (frequency bands 1 to 3), and the energy is further concentrated in the low-frequency band in the intermediate zone and zone far from the blasting source. There is a distortion process in which the vibration velocity and the main frequency increase slightly and the energy of the blasting vibration wave converges to the high-frequency band (the 5th band) before the sudden unstable fracture failure of the specimens. The experimental results indicate that the prediction and evaluation of blasting vibration should consider the variation rule of blasting vibration wave parameters synthetically based on the cumulative damage effect, and it is not safe to use only one fixed vibration control standard for the whole blasting operation.

1. Introduction

In the rapid process of development of infrastructure construction in China, the blasting technique is widely adopted as an effective method during construction in the transportation, mining, municipal, hydropower, nuclear power, and other industries [1–3].

Unfortunately, only about 20% of the energy released is utilized to fragment and displace the rock mass; the rest of the energy is wasted and produces undesirable environmental damages [4–9], such as ground vibration, fly rock, air shock waves, dust, and back-break. Blasting ground vibration is one of the most fundamental of these environmental damages, and high blast vibrations can cause damage to structures and nearby residential areas [10, 11]. Therefore, the environmental damage induced by blasting ground vibration is always a difficult and hot problem in the blasting field.

In blasting engineering practice, some blasting projects usually require frequent and multiple blasting operations, such as in tunnel and underground space blasting excavation construction, quarry blasting construction, and so on; therefore, the ground vibration damage accumulation effect is inevitable [12–15], and the damage accumulation effects will inevitably affect the propagation and attenuation of the ground vibration wave.

A great deal of research work focused on the adverse effects of blasting ground vibration has been carried out by scholars around the world, and the prediction and control of blasting ground vibration are the central topic of study.

Statistical methods [16–23] based on field and experimental test data of blasting ground vibration are the main method of summarizing the empirical equations. At the same time, besides the statistical methods, some new methods are used to explore the prediction and control of blasting ground vibration in the literature, such as the soft computing method [24–27]. The artificial neural network (ANN) method [28–31], known as flexible nonlinear function approximation, has been widely used to predict the ground vibration too, but the ANN method should be based on a large number of in situ monitoring data.

It can be seen from the above that many researchers have studied the prediction and control of blasting ground vibration. However, the studies are almost all based on single blasting operations, while the damage accumulation effect of blasting vibration is rarely considered. Moreover, the propagation and attenuation rule of the blasting ground vibration wave from the blast to nearby areas is the most important foundation of blasting vibration prediction and control. Therefore, it is necessary to carefully study the propagation and attenuation rule of blasting vibration wave parameters based on the damage accumulation effect to ensure the accuracy of vibration prediction and the effectiveness of vibration control measures.

In this paper, we pay more attention to the influence of damage accumulation effects on the propagation rule of the vibration wave. A blasting vibration damage accumulation experiment was carried out, and the propagation rule of the blasting vibration wave parameters (vibration velocity, main frequency, and energy) was found. The results obtained in this study will lead to a better understanding of the propagation and attenuation rule of blasting vibration wave parameters (vibration velocity, main frequency, and energy) with the increase in the number of blasts.

2. Experimental Method

In the laboratory of Henan Polytechnic University in China, experimental specimens with dimensions of 1500 mm × 500 mm × 300 mm were cast for the blasting vibration damage accumulation experiment, as shown in Figure 1(a), and three specimens were tested to obtain the average results to minimize the uncertainty. Natural river sand with a fineness modulus of 2.9 was selected as the fine aggregate and cleaned gravel with a maximum size of 8 mm was selected as the coarse aggregate. The concrete mix proportions are given in Table 1.

The specimens were made with a blasthole in them, the diameter and the depth of the blasthole are 16 mm and 180 mm, respectively, the explosive charge is designed as 2.5 g (the peak compressive strain at the blasthole wall that fails to cause crushing) in single blasting experiment, and the explosive selected is passivated hexogeon (RDX).

In the course of the experiment, the vibration wave was monitored on the surface of specimens by using a TC-4850 blasting vibration meter (Chendu Zkck Tech Co., Ltd.). The horizontal distances between each monitoring point and the centre of the blasthole were 5, 15, 35, 55, 75, 95, and 105 cm, respectively, as shown in Figure 1(b). At the same time, the ultrasonic wave velocity of the specimens was measured by an NM-4A ultrasonic detector (Beijing Zhongtuo Tech Co., Ltd.) before and after the blasting test, as shown in Figure 1(c), and the damage values were calculated using the formula $D = 1 - (v/v_0)^2$, where v_0 is the ultrasonic wave velocity of virgin specimens (km/s) and v is the ultrasonic wave velocity of specimens to which the vibration load has been applied (km/s). A total of 11 measuring points were arranged in the horizontal direction, the interval distance between two adjacent measuring points (mp) was 100 mm, and the first measuring point was 50 mm from the centre of the blasthole. The test continued until fracture failure of the specimens. In order to weaken the influence of the boundary effect on the test results, the specimens were coated with 2 cm-thick butter and clamped with steel plates, as shown in Figure 1(b).

3. Results and Discussion

Three concrete specimens experienced fracture failure after the 10th, 11th, and 9th blasts, respectively; therefore, only the results of nine blasting tests are analysed in this work, and the average values of ultrasonic wave velocity and blasting vibration parameters of three test blocks are taken as the final test results to minimize the uncertainty. The energy calculation and analysis are based on the experimental results of the 9th blasting vibration wave.

3.1. Damage Study of the Specimens after the Blasting Experiment. Table 2 gives the calculation results of the blasting damage value after each blasting experiment, and the curves of the cumulative damage value versus the number of blasts are shown in Figure 2.

According to the data in Table 2, the relationship between the damage accumulation value and the ratio of number of blasting cycles can be obtained, as shown in Formula (1):

$$D_i(x_i) = ax_i^3 + bx_i^2 + cx_i, \quad (1)$$

where D_i is the damage accumulation value after blasting, x_i is the ratio of number of blasting cycles under the same charge, $x_i = i/N$, N is the total number of blasts, $a, b,$ and c are constants, and $a \neq 0$.

At the same time, using the test results in Table 2 to judge the monotonicity of the formula, it was found that Formula (1) is a monotonically increasing function under the experimental condition. Then, from Table 2, Figure 2, and Formula (1), it could be obtained directly that the damage values of all measured points increase with the increase of the number of blasts.

In the zone near to the blasting source (7–150R_0, where R_0 is the radius of charge), the damage value and damage range are directly determined by the intensity and attenuation velocity of the explosive stress wave and explosive gas [32]. When the number of blasts was less, the damage value was larger and increased rapidly. However, the amount of charge remained constant during the test, and the degree and range of damage to the specimen increased with the increase in the number of blasts, the stress wave attenuated quickly [33], and the explosion gas pressure quickly

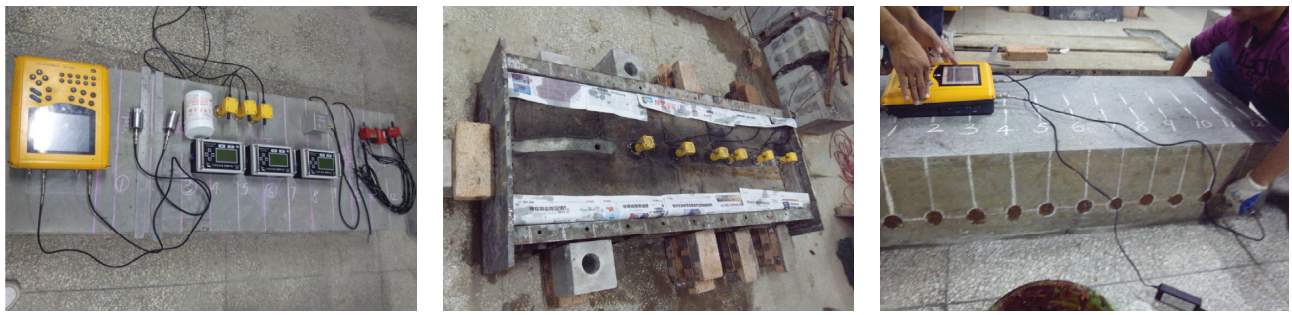

(a) (b) (c)

Figure 1: Experimental pictures.

Table 1: Mix proportions of the studied concrete.

Concrete	Water/cement ratio	Cement (kg/m^3)	Water (kg/m^3)	Sand (kg/m^3)	Gravel (kg/m^3)
C40	0.49	479.6	235	691.0	994.4

Table 2: Blast damage results.

Number of blasts	Monitoring point										
	1	2	3	4	5	6	7	8	9	10	11
1	0.023	0.003	0.008	0	0.014	0.011	0.005	0.008	0	0	0
2	0.037	0.013	0.008	0.002	0.022	0.017	0	0.008	0	0	0
3	0.058	0.024	0.01	0	0.022	0.014	0	0.016	0	0	0
4	0.074	0.037	0.017	0.009	0.028	0.008	0.008	0.016	0.001	0.001	0
5	0.084	0.049	0.033	0.017	0.019	0.008	0.008	0.016	0.003	0.002	0.003
6	0.104	0.064	0.041	0.023	0.027	0.015	0.008	0.019	0.006	0.004	0.005
7	0.163	0.151	0.1	0.064	0.035	0.023	0.017	0.021	0.008	0.005	0.006
8	0.176	0.165	0.151	0.105	0.074	0.031	0.025	0.033	0.009	0.007	0.008
9	0.195	0.185	0.178	0.154	0.142	0.11	0.105	0.09	0.011	0.01	0.009

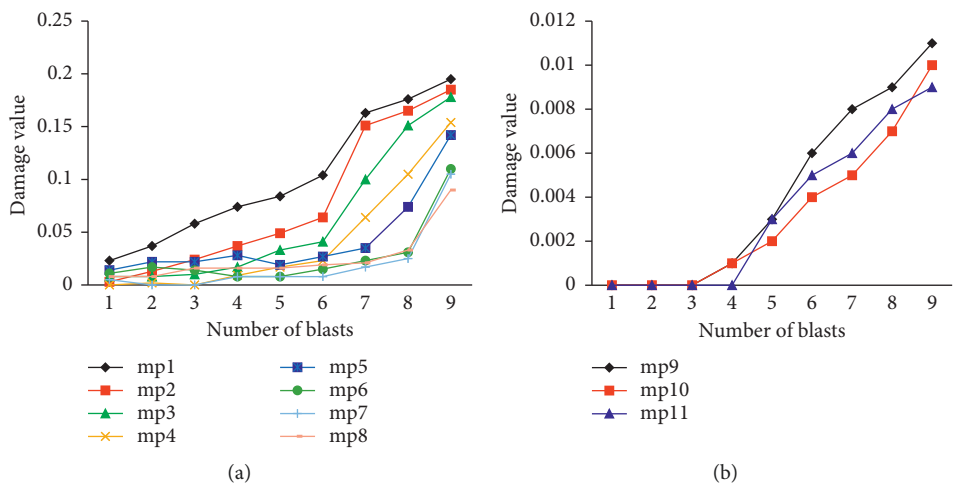

(a) (b)

Figure 2: Curves of cumulative damage value versus the number of blasts.

decreased too, so the damage increased slowly with the continuous increase in the number of blasts.

With the increase of the distance from the centre of the blasthole (greater than $150R_0$), the explosion stress wave and explosion gas can only cause indirect damage to the specimen [34]. Due to stress concentration, microcosmic local plastic deformation occurs at the crack tip. This kind of local plastic deformation continuously accumulates with the increase in the number of blasts. When the dynamic stress intensity factor $K_{I(t)}$ at the crack tip increases to the critical value of crack growth $K_{\mathrm{ID}}^{\mathrm{ini}}$, the crack begins to expand and gradually forms a mesocrack. At this stage, the damage increases slowly with the increase in the number of blasts.

If the number of blasts continues to increase, the dynamic stress intensity factor $K_{I(t)}$ at the crack tip accumulates until it reaches to the dynamic fracture toughness $K_{\mathrm{ID}}^{\mathrm{um}}$ of the specimen. The microcracks gradually penetrate and form macroscopic cracks, and the crack growth rate accelerates in the form of instability. At this stage, the damage begins to increase rapidly, and a process of mutation may even occur.

3.2. The Propagation and Attenuation Rule of Blasting Vibration Wave Parameters

3.2.1. The Propagation and Attenuation Rule of the Vibration Velocity and Main Frequency. Table 3 gives the results of blasting vibration velocity and main frequency, and Figure 3 shows the variation curves of vibration velocity and main frequency with the increase in the number of blasts.

In order to better understand the variation rule of particle vibration velocity, the main frequency, and the damage accumulation with the increase in the number of blasts and the corresponding relationship between them, the vibration velocity and the damage accumulation were increased 100-fold and 10000-fold, respectively, without regard to dimensional units, and then the variation curves of vibration velocity, main frequency, and damage accumulation with the increase in the number of blasts were obtained. The variation curves of monitoring points 1, 5, and 7 were obtained as shown in Figure 4.

From Table 3 and Figure 4, it can be seen that the velocity and main frequency of blasting vibration decrease continuously with the increase in the number of blasts, and there is a good linear relationship between them. However, the variations of vibration velocity and main frequency show the opposite trend to the damage accumulation of blasting.

According to the analysis presented in Section 3.1, the damage value of the specimen increases with the increase in the number of blasts; that is to say, the number and length of weak planes such as cracks in the test block increase, so the frequency and probability of reflection, refraction, and scattering in the process of vibration wave propagation are increased, all of which increases the propagation path of the vibration wave, and thus the vibration velocity is inevitably reduced. Therefore, the vibration velocity of the monitoring point decreases with the increase in the number of blasts.

At the same time, all kinds of structurally weak surfaces play the role of low-pass filter. The high-frequency component of the blasting vibration wave is gradually absorbed, and the proportion of the low-frequency component increases, so the main frequency of blasting vibration decreases continuously. There is a good linear relationship between the velocity and the main frequency of vibration.

3.2.2. The Propagation and Distribution of Blasting Vibration Wave Energy. In order to analyse the energy propagation and distribution of the blasting vibration wave based on the damage accumulation effects, the wavelet basis function (error order 10–12) is used to decompose and reconstruct the measured blasting vibration signal with a scale of 8, and then the energy of the nine decomposed frequency bands is calculated. The nine frequency bands are 0–15.625, 15.625–31.25, 31.25–62.5, 62.5–93.75, 93.75–125, 125–187.5, 187.5–250, 250–375, and 375–500 Hz, respectively. Finally, the ratio of the energy of each frequency band to the total energy is calculated. The calculated results of blasting vibration wave energy are given in Table 4.

According to the data in Table 4, the energy distribution curve of monitoring points 1, 5, and 7 for each blast can be obtained, as shown in Figures 5(a)–5(c). The change curves of the energy concentrated in the low-frequency band (bands 1 to 3) with the increase in the number of blasts are shown in Figure 5(d).

(1) From Table 4 and Figure 5, it can be seen that the energy distribution of the blasting vibration wave is scattered in the zone near to the blasting source, but with the increase in the number of blasts, the energy distribution of the blasting vibration wave is mainly concentrated in the low-frequency band. In the intermediate zone and the zone far from the blasting source, the energy of the blasting vibration wave is mainly concentrated in the low-frequency band.

A blasting vibration wave is a kind of transient wave and random wave, so it is a broadband wave with different frequencies. The main frequency of blasting vibration attenuates rapidly with the increase of the distance from the measuring point to the blasting centre and the degree of damage to the propagation medium.

In the zone near to the blasting source, when number of blasts is smaller, the blasting damage value is small too, and the high-frequency filtering effect on the weak plane of the structure such as cracks is not obvious. The energy of blasting vibration is distributed in different frequency bands, so the energy distribution is relatively dispersed and the proportion of energy concentrated in the low-frequency band is lower. However, with the increase in the number of blasts, the high-frequency filtering effect of the weak plane of the structure is enhanced, the high-frequency component decreases rapidly, and the energy of the low-frequency band increases rapidly after the damage continues to increase. The main frequency of the vibration decreases with the increase of the distance [35, 36], so in the intermediate zone and the zone far from the blasting source, the energy of the vibration wave is concentrated in the low-frequency band and the energy of frequency bands 1 to 3 represents more than 85% of the total energy. If the blasting times continue to increase, the damage value of the specimens will continue to increase too and the high-frequency filtering effect will be more obvious, so the main frequency decreases and the energy of the blasting vibration wave will be further concentrated in the low-frequency band.

(2) From Figures 4 and 5, it can be seen that there is a distortion process in which the vibration velocity and the main frequency increase slightly and the energy of the blasting vibration wave converges to the high-frequency band (the 5th band) before the sudden unstable fracture failure.

After the mesoscopic crack passes through and forms a macroscopic crack, the crack growth rate accelerates in the form of instability [34, 37], and the number of microcracks

Table 3: The results of blasting vibration velocity (cm/s) and main frequency (Hz).

Number of blasts	Monitoring point						
	1	2	3	4	5	6	7
1	17.04/499.99	9.81/379.95	7.50/333.35	3.94/249.99	2.54/216.66	2.28/201.43	1.68/189.99
2	11.86/481.96	8.68/333.35	6.53/313.32	2.93/226.66	2.02/201.43	1.72/199.99	0.88/164.44
3	9.60/433.35	5.04/296.31	3.64/283.01	2.48/200.00	0.94/182.13	0.69/179.99	0.63/153.63
4	6.60/403.36	4.15/269.99	2.97/250.00	2.14/184.44	0.71/163.63	0.64/150.00	0.49/138.47
5	6.00/385.35	4.03/251.01	3.05/239.99	1.86/169.99	0.92/145.71	0.69/136.66	0.42/121.21
6	5.98/357.31	3.70/236.00	2.60/216.66	1.60/153.33	0.66/125.29	0.60/116.66	0.45/101.21
7	5.69/329.99	1.94/216.66	2.36/204.44	1.34/137.69	0.63/110.52	0.69/98.14	0.27/70.90
8	**5.72/319.00**	**3.44/236.66**	**3.29/217.66**	**2.03/141.71**	**1.74/125.47**	**1.50/102.11**	**1.01/83.72**
9	3.60/280.00	1.64/199.99	1.33/179.65	0.90/112.22	0.77/91.11	0.46/61.42	0.35/41.57

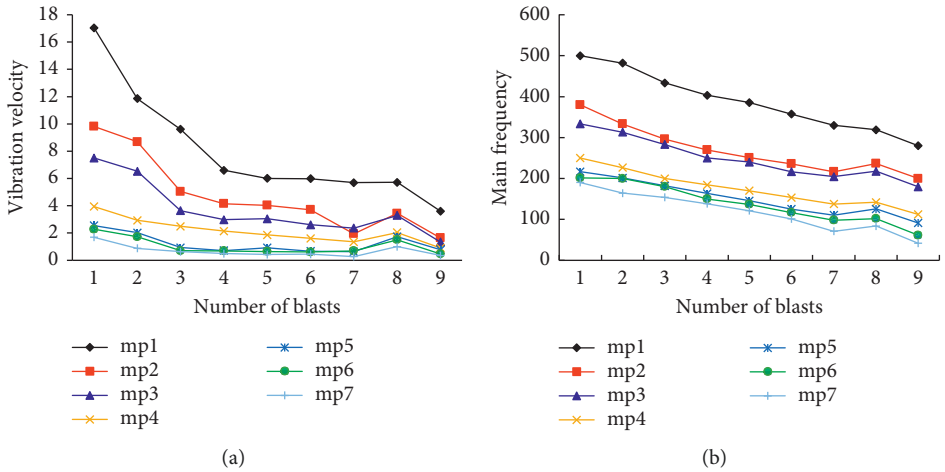

Figure 3: Change curves of vibration velocity and main frequency with the increasing in the number of blasts.

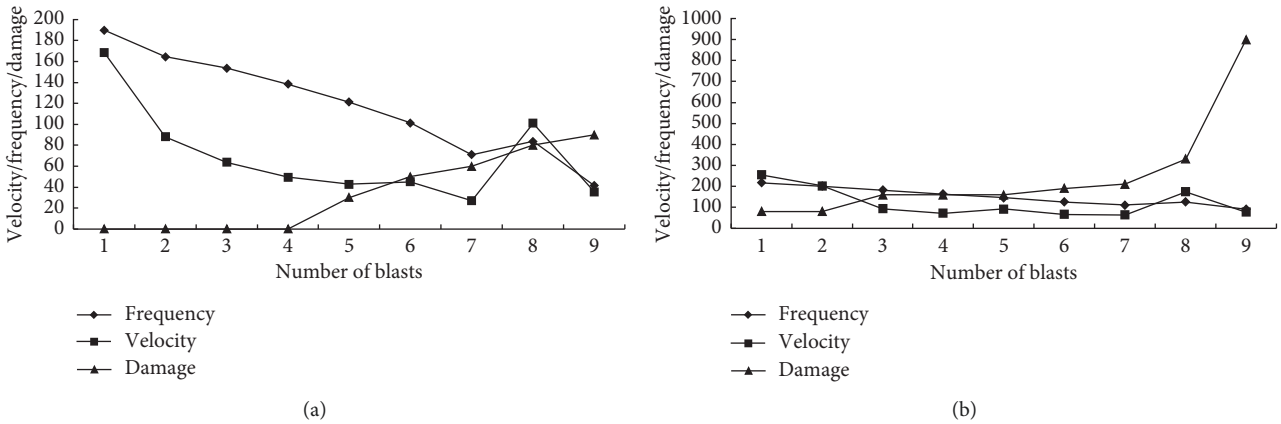

Figure 4: Continued.

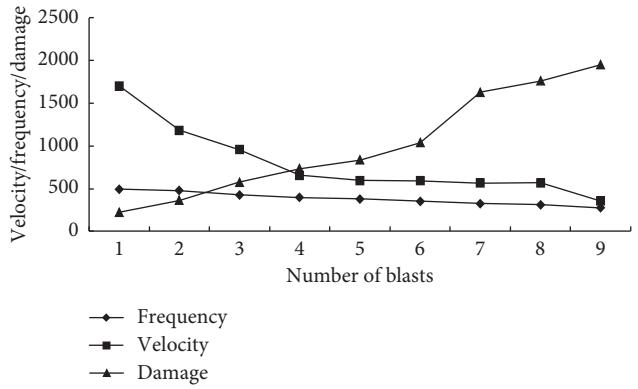

(c)

Figure 4: Curves of the relations between the main frequency, velocity, and damage accumulation of blasting vibration.

Table 4: The calculated results of blasting vibration wave energy.

Frequency band	Number of blasts								
	1	2	3	4	5	6	7	8	9
1	0.4428	0.3883	0.4573	0.3471	0.4276	0.4332	0.4665	0.4383	0.4266
2	0.3206	0.391	0.3348	0.4161	0.3481	0.3485	0.3527	0.3592	0.3513
3	0.0984	0.1086	0.0783	0.1091	0.1022	0.1012	0.0641	0.1002	0.1629
4	0.0533	0.0513	0.0753	0.0712	0.0619	0.0702	0.0664	0.0319	0.0201
5	0.0439	0.0413	0.0205	0.0251	0.0232	0.0172	0.0149	0.0511	0.0205
6	0.0237	0.0112	0.0208	0.0171	0.0204	0.018	0.0122	0.0017	0.0008
7	0.0062	0.0011	0.0041	0.003	0.005	0.0036	0.0057	0.0008	0.0029
8	0.0013	0.0012	0.001	0.0022	0.0032	0.0006	0.0092	0.0087	0.0077
9	0.0098	0.006	0.0079	0.0091	0.0084	0.0075	0.0083	0.0081	0.0072
Sum energy of 1–3 band	0.8618	0.8879	0.8704	0.8723	0.8779	0.8829	0.8833	0.8977	0.9408

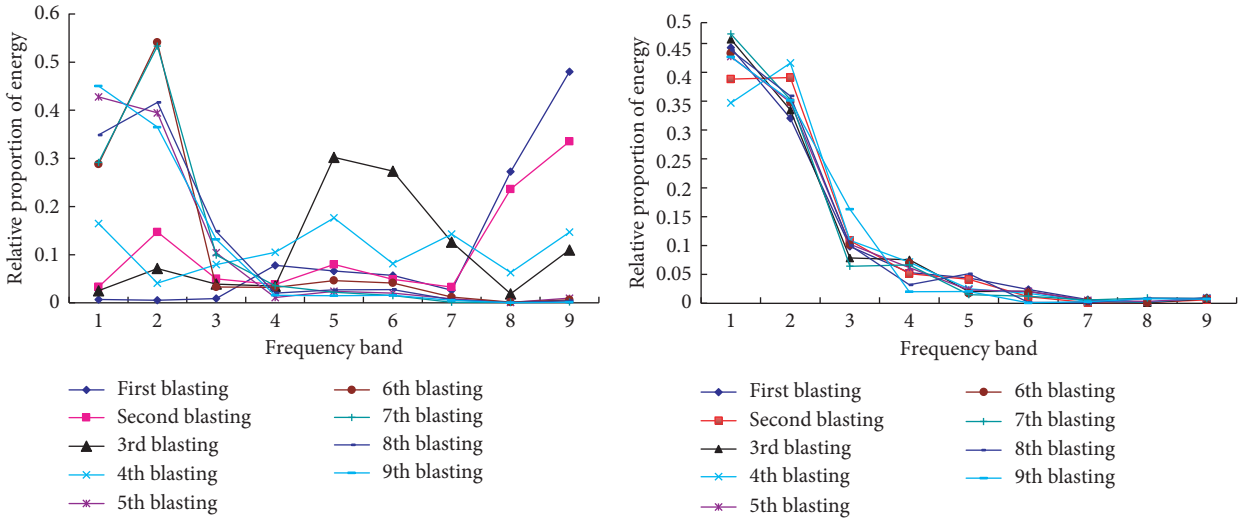

(a) (b)

Figure 5: Continued.

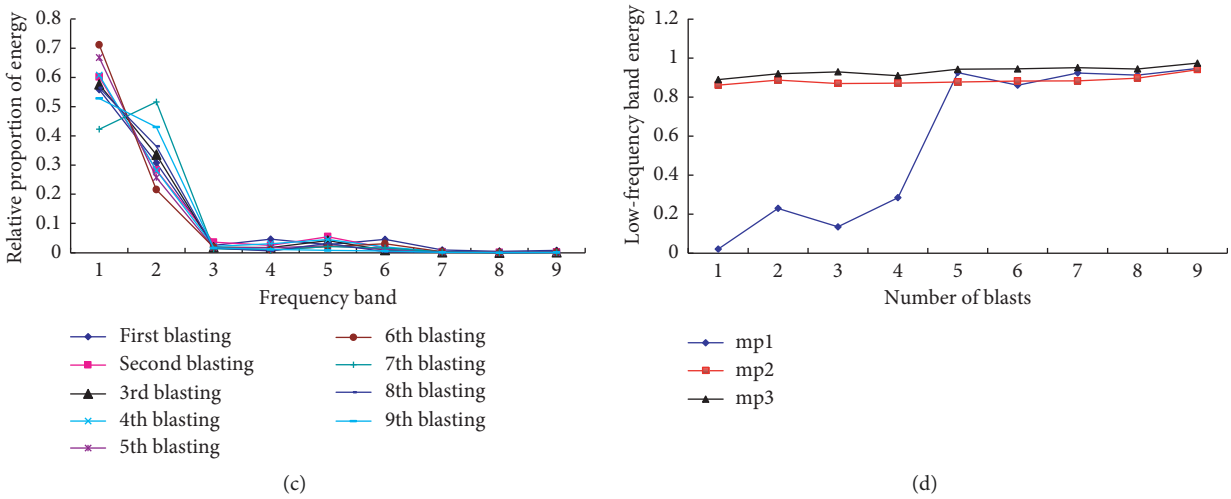

Figure 5: Distribution curves of blasting vibration wave energy.

decreases in the process of macroscopic crack growth, so the high-frequency filtering effect of the sample block is weakened. At this stage, there is less energy available to expand the macrocrack [34, 37] and more of the energy carried by the stress wave is converted into vibration wave energy. So, the vibration velocity and the main frequency of the measuring point suddenly increase before fracture failure of the test block, and the energy of vibration wave is concentrated in the high-frequency band (band 5). Subsequently, the stress wave energy leaks along the macroscopic crack, the particle vibration velocity and the main frequency decrease, and the vibration wave energy is concentrated in the low-frequency band.

4. Conclusions

The main objective of this study is to reveal the propagation and attenuation rule of blasting vibration wave parameters based on the damage accumulation effect. Based on the test results and discussion presented in this study, the following conclusions can be drawn:

(1) The blasting damage increases continuously with the increase in the number of blasts and there is a cubic polynomial function relationship between the damage accumulation of blasting and the ratio of number of blasting cycles. However, the velocity and frequency of blasting vibration decrease continuously with the increase in the number of blasts and there is a good linear relationship between them, but the trends of the variations of vibration velocity and main frequency are contrary to that of the damage accumulation of blasting.

(2) In the zone near to the blasting source, the energy distribution of the blasting vibration wave is scattered, but in the intermediate zone and the zone far from the blasting source, the energy distribution of the blasting vibration wave is mainly concentrated in the low-frequency band, and with the increase in the number of blasts, the energy distribution of the blasting vibration wave is mainly concentrated in the low-frequency band.

(3) In the process of macroscopic crack expansion, there is a distortion process in which the vibration velocity and the main frequency increase slightly and the energy of the blasting vibration wave converges to the high-frequency band (the 5th band) before the sudden unstable fracture failure.

(4) In practice, if the damage accumulation effect exists, it is not safe to use only one fixed vibration control standard for the whole blasting operation, and the prediction and evaluation of blasting ground vibration should consider the propagation and attenuation rule of blasting vibration wave parameters synthetically based on the damage accumulation effect.

Data Availability

The data used to support the findings of this study are included within the article.

Conflicts of Interest

The authors declare that they have no conflicts of interest.

Acknowledgments

This work is supported by the Chinese National Natural Science Foundation (grant numbers 11542019 and 51504082) and Henan Research Program of Foundation and Advanced Technology (grant number 162300410032). The authors wish to express their thanks to all supporters.

References

[1] W. B. Lu, Y. Luo, M. Chen et al., "An introduction to Chinese safety regulations for blasting vibration," *Environmental Earth Sciences*, vol. 67, no. 7, pp. 1951–1959, 2012.

[2] M. Hajihassani, D. J. Armaghani, M. Monjezi et al., "Blast-induced air and ground vibration prediction: a particle swarm

optimization-based artificial neural network approach," *Environmental Earth Sciences*, vol. 74, no. 4, pp. 2799–2817, 2015.

[3] N. Jiang and C. B. Zhou, "Blasting vibration safety criterion for a tunnel liner structure," *Tunnelling and Underground Space Technology*, vol. 32, pp. 52–57, 2012.

[4] P. Segarra, J. F. Domingo, L. M. López, and J. A. Sanchidrián, "Prediction of near field overpressure from quarry blasting," *Applied Acoustics*, vol. 71, no. 12, pp. 1169–1176, 2010.

[5] M. Monjezi, H. A. Khoshalan, and A. Y. Varjani, "Prediction of flyrock and backbreak in open pit blasting operation: a neurogenetic approach," *Arabian Journal of Geosciences*, vol. 5, no. 3, pp. 441–448, 2012.

[6] D. J. Armaghani, M. Hajihassani, E. T. Mohamad, A. Marto, and S. A. Noorani, "Blasting-induced flyrock and ground vibration prediction through an expert artificial neural network based on particle swarm optimization," *Arabian Journal of Geosciences*, vol. 7, no. 12, pp. 5383–5396, 2014.

[7] A. Marto, M. Hajihassani, D. J. Armaghani, E. T. Mohamad, and A. M. Makhtar, "A novel approach for blast-induced flyrock prediction based on imperialist competitive algorithm and artificial neural network," *Scientific World Journal*, vol. 2014, Article ID 643715, 11 pages, 2014.

[8] M. Movahedi, A. H. Kokabi, S. M. S. Reihani, W. J. Cheng, and C. J. Wang, "Prediction and optimization of back-break and rock fragmentation using an artificial neural network and a bee colony algorithm," *Bulletin of Engineering Geology and the Environment*, vol. 75, no. 1, pp. 27–36, 2016.

[9] M. Monjezi, H. A. Mohamadi, B. Barati, and M. Khandelwal, "Application of soft computing in predicting rock fragmentation to reduce environmental blasting side effects," *Arabian Journal of Geosciences*, vol. 7, no. 2, pp. 505–511, 2014.

[10] S. O. Olofsson, *Applied Explosives Technology for Construction and Mining*, Applex, Sweden, 1988.

[11] T. N. Singh and V. Singh, "An intelligent approach to prediction and control ground vibration in mines," *Geotechnical and Geological Engineering*, vol. 23, no. 3, pp. 249–262, 2005.

[12] J. H. Yang, W. B. Lu, Y. G. Hu, M. Chen, and P. Yan, "Accumulated damage in surrounding rocks due to repeated blasting loads during blasting excavation of tunnels," *Rock and Soil Mechanics*, vol. 35, no. 2, pp. 511–518, 2014.

[13] J. Liu and Q. H. Cui, "Advances in methods of predicting blasting-induced vibrations," *Journal of Hehai University (Natural Sciences)*, vol. 43, no. 5, pp. 465–471, 2015.

[14] C. S. Wu, G. H. Li, K. Y. Guo et al., "Research on accumulated vibration effects of surrounding rock in blasting excavating anchorage tunnel for suspension bridge," *Chinese Journal of Rock Mechanics and Engineering*, vol. 28, no. 7, pp. 1499–1505, 2009.

[15] Y. M. Li, Z. G. Gao, Q. Q. Zhu et al., "An experimental investigation into effects of blast-induced vibration on strength of early-age concrete," *Explosion and Shock Waves*, vol. 33, no. 3, pp. 243–248, 2013.

[16] L. Ahmed and A. Ansell, "Vibration vulnerability of shotcrete on tunnel walls during construction blasting," *Tunnelling and Underground Space Technology*, vol. 42, pp. 105–111, 2014.

[17] M. Khandelwal, "Blast-induced ground vibration prediction using support vector machine," *Engineering with Computers*, vol. 27, no. 3, pp. 193–200, 2011.

[18] K. Dey and V. M. S. R. Murthy, "Prediction of blast-induced overbreak from uncontrolled burn-cut blasting in tunnels driven through medium rock class," *Tunnelling and Underground Space Technology*, vol. 28, no. 1, pp. 49–56, 2012.

[19] R. Nateghi, "Prediction of ground vibration level induced by blasting at different rock units," *International Journal of Rock Mechanics and Mining Sciences*, vol. 48, no. 6, pp. 899–908, 2011.

[20] T. Hudaverdi, "Application of multivariate analysis for prediction of blast-induced ground vibrations," *Soil Dynamics and Earthquake Engineering*, vol. 43, pp. 300–308, 2012.

[21] G. L. Yang, R. S. Yang, and Y. L. Che, "Damage accumulative effect of surrounding rock under periodic blasting vibration," *Journal of China Coal Society*, vol. 38, no. s1, pp. 25–29, 2013.

[22] H. L. Fei, S. K. Wang, and Z. G. Yang, "Blasting damage study on rock slope in opencast coal mine," *Blasting*, vol. 31, no. 2, pp. 51–56, 2014.

[23] H. L. Fei and X. P. Zhao, "Experimental study on damage accumulation in rock slope caused by blasting vibration," *Blasting*, vol. 26, no. 4, pp. 1–3, 2009.

[24] M. Khandelwal and T. N. Singh, "Prediction of blast induced ground vibrations and frequency in opencast mine: a neural network approach," *Journal of Sound and Vibration*, vol. 289, pp. 711–725, 2006.

[25] M. T. Mohamed, "Performance of fuzzy logic and artificial neural network in prediction of ground and air vibrations," *International Journal of Rock Mechanics and Mining Sciences*, vol. 48, no. 5, pp. 845–851, 2011.

[26] M. Monjezi, M. Ahmadi, A. Sheikhan, M. Bahrami, and A. R. Salimi, "Predicting blast-induced ground vibration using various types of neural networks," *Soil Dynamics and Earthquake Engineering*, vol. 30, no. 11, pp. 1233–1236, 2010.

[27] M. Monjezi, M. Ghafurikalajahi, and A. Bahrami, "Prediction of blast-induced ground vibration using artificial neural networks," *Tunnelling and Underground Space Technology*, vol. 26, no. 1, pp. 46–50, 2011.

[28] D. J. Armaghani, M. Hajihassani, B. Y. Bejarbaneh, A. Marto, and E. T. Mohamad, "Indirect measure of shale shear strength parameters by means of rock index tests through an optimized artificial neural network," *Measurement*, vol. 55, pp. 487–498, 2014.

[29] E. Momeni, D. J. Armaghani, M. Hajihassani, and M. F. M. Amin, "Prediction of uniaxial compressive strength of rock samples using hybrid particle swarm optimization-based artificial neural networks," *Measurement*, vol. 60, pp. 50–63, 2015.

[30] M. Hajihassani, D. J. Armaghani, H. Sohaei, E. T. Mohamad, and A. Marto, "Prediction of airblast-overpressure induced by blasting using a hybrid artificial neural network and particle swarm optimization," *Applied Acoustics*, vol. 80, pp. 57–67, 2014.

[31] E. Ghasemi, M. Ataei, and H. Hashemolhosseini, "Development of a fuzzy model for predicting ground vibration caused by rock blasting in surface mining," *Journal of Vibration and Control*, vol. 19, no. 5, pp. 755–770, 2013.

[32] X. L. Yang and S. R. Wang, "Meso-mechanism of damage and fracture on rock blasting," *Explosion and Shock Waves*, vol. 20, no. 3, pp. 247–252, 2000.

[33] H. B. Chu, H. Y. Ye, X. L. Yang et al., "Experimental research on propagation rule of blasting vibration based on the damage accumulation," *Journal of Vibration and Shock*, vol. 35, no. 2, pp. 173–177, 2016.

[34] C. B. Yan, G. J. Wang, Q. W. Wang et al., *Research on the Cumulative Blasting Damage Effect and Dynamic Instability of Rock*, The Yellow River Water Conservancy Press, Zhengzhou, China, 2011.

[35] F. Q. Gao, A. J. Hou, X. L. Yang et al., "Analysis of blasting vibration frequency based on dimensional method," *Blasting*, vol. 27, no. 3, pp. 1–8, 2010.

[36] S. B. Chai, J. C. Li, and L. F. Rong, "Theoretical study for induced seismic wave propagation across rock masses during underground exploitation," *Geomechanics and Geophysics for Geo-Energy and Geo-Resources*, vol. 3, no. 2, pp. 95–105, 2017.

[37] C. Y. Li, Y. P. Song, and Y. Che, "Study on damage accumulation behavior of concrete under uniaxial cyclic load," *China Civil Engineering Journal*, vol. 35, no. 2, pp. 38–40, 2002.